

Compact Passive Devices in InP Membrane on Silicon

F. Bordas⁽¹⁾, G. Roelkens⁽²⁾, R. Zhang⁽¹⁾, E. J. Geluk⁽¹⁾, F. Karouta⁽¹⁾, J.J.G.M. van der Tol⁽¹⁾, P.J. van Veldhoven⁽¹⁾, R. Nötzel⁽¹⁾, D. Van Thourhout⁽²⁾, R. Baets⁽²⁾ and M.K. Smit⁽¹⁾

⁽¹⁾ COBRA Research Institute, Technische Universiteit Eindhoven, P.O. Box 513, NL-5600MB Eindhoven
F.Bordas@tue.nl

⁽²⁾ Photonics Research Group, Ghent University-IMEC, Ghent, Belgium
gunther.roelkens@intec.ugent.be

Abstract *The high vertical index contrast and the small thickness of thin InP membranes (200nm) bonded with BCB allow the achievement of very small devices. In this paper we will present some performances of such photonic integrated circuit building blocks (wires, 3dB splitters and ring resonators).*

Introduction

The complexity of photonic integrated circuits (PICs) has raised these last years, following Moore's law. But to satisfy the need for even further complexity, devices and waveguides have to be made smaller and less power consuming. One of the solutions for this is to use membranes, so the waveguide layer has a high vertical index contrast. Suspended membranes have the highest vertical index contrast, as they are surrounded with air. However this solution is hard to handle for a complete PIC. Lot of work has been reported about bonded membranes, mainly Silicon On Insulator (SOI). Silicon is an ideal candidate for passive devices, but this material does not allow the achievement of integrated active devices. III-V semiconductors can handle both passive and active functionalities, which make them good candidates for non-heterogeneous active-passive integration. Our work concerns thin InP membranes bonded with BCB on Si. We will first present the performances of basic circuitry building blocks, such as wires and 3dBsplitters. Then some results about ring resonator notch filters will be presented. The chip is first processed on an epitaxial InP and quaternary layer structure. Then, the sample is bonded with BCB¹ and the substrate and sacrificial layers are removed so that only the 200nm thick patterned InP membrane is left. The whole fabrication process is described elsewhere². Light is coupled into and extracted from the chip using compact grating couplers^{3,4}.

Wires

The fabricated wires are 400nm wide. In a first set of experiments the different lengths were 50, 100, 300

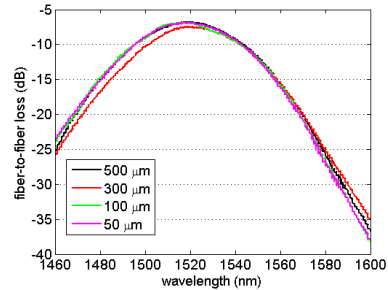
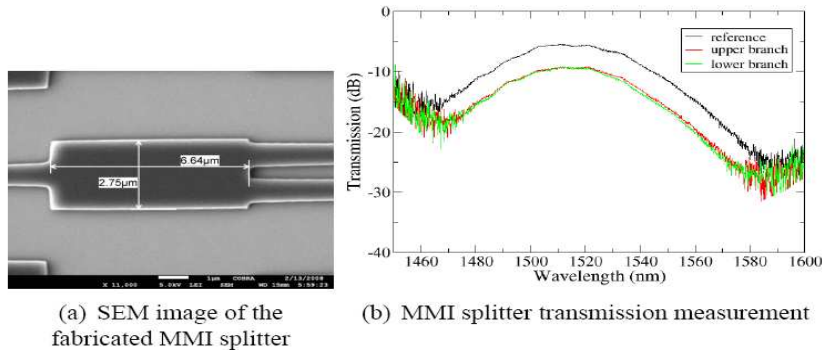


Fig. 1: Fiber-to-fiber transmission through wires of different lengths

and 500 μm . Fiber-to-fiber losses are reported on fig.1. The difference between the different curves is less than 0.5 dB, which gives an upper value for propagation losses of 10 dB/cm. This losses value is higher than the one reported for similar wires in SOI⁵, but can still be improved. Moreover, they are comparable to losses achieved in wide deeply etched III-V waveguides⁶. Similar performances have been achieved in⁷ for InP wires in the same configuration.

3dB splitter

3dB-splitters are also a building block of circuitry in PICs. We fabricated an ultra-small 1×2 -MMI splitter (less than $20 \mu\text{m}^2$) and measured the transmission through each output branch while using the same input for both. The reference is a 50 μm long wire. Transmission measurements are reported figure 2(b), and a SEM image of the device is shown figure 2(a). The transmissions through each branch are the same, 3.6 dB lower than for the reference. This device is to our knowledge the smallest 3dB-splitter ever reported, and excess losses are only 0.6 dB.



(a) SEM image of the fabricated MMI splitter

(b) MMI splitter transmission measurement

Fig. 2: MMI splitter characterization

Ring resonators

We also fabricated ring resonator notch filters. The measured transmission spectrum for a ring resonator with a radius of $4\ \mu\text{m}$ and a fabricated gap of $150\ \text{nm}$ is shown in fig. 3, revealing a free spectral range (FSR) of $28.2\ \text{nm}$. The resonance at $\lambda=1603.5\ \text{nm}$ as an extinction ratio of $16\ \text{dB}$ and the loaded Q-factor, defined as f_0/FWHM with f_0 the central frequency and FWHM the full width half maximum, is then 5830 .

The asymmetric form of the curve indicates non-linear effects, similar to the behaviour of SOI ring resonators⁸. Therefore, we have measured the transmission spectrum of the ring resonator structure for increasing input power of the tunable laser. The result is shown in fig. 4. For the lowest input powers, the resonance wavelength is slightly blue shifted as the input power is increased. For higher input powers, a wavelength red shift and bistability occurs. This can be explained as follows. Due to two photon absorption free carriers are generated, resulting in additional absorption (free carrier absorption) and an associated negative refractive index change due to free carrier dispersion. Recombination of these carriers results in heating and a positive thermal refractive index change. For the lower input powers, the free carrier dispersion effect is dominant, resulting in a blue shift of the resonance. For higher input powers, the thermal effects take over, resulting in a wavelength red shift and eventually bistability.

For the SOI ring resonators in⁸, thermal effects are dominant for all input powers and only a red shift of the resonance is observed. In⁹, where III-V material is bonded onto SOI racetrack resonators, the blue shift due to free carrier dispersion is also observed.

A second set of rings has been fabricated in the same way. A fit of the experimental data for one of the peak of a $14\ \mu\text{m}$ diameter ring, centred around $\lambda=1530\ \text{nm}$, shown in Fig. 5, allowed us to extract values for Q above $15,000$ and α (propagation losses in the ring) $\sim 7\ \text{dB/cm}$. These losses correspond to those measured on straight wires, and the Q value is very promising as it ensures lasing action with active material.

Conclusions

We fabricated and characterized very compact and

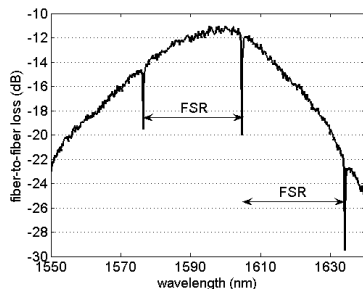


Fig. 3: Fibre-to-fibre transmission through the bus waveguide at low input power

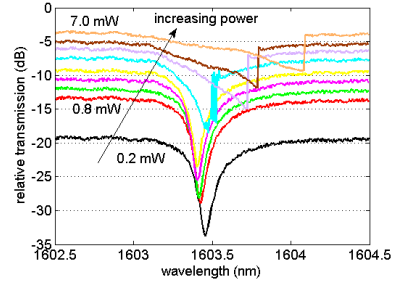


Fig. 4: Resonance at $\lambda=1603.5\ \text{nm}$ for increasing input powers, resulting in bistability.

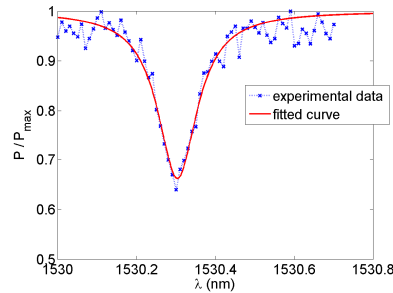


Fig. 5: Experimental and fitted curves of the peak at $1530\ \text{nm}$ for the second set of rings.

low-loss straight and bended wires, together with an ultra-compact $3\ \text{dB}$ -splitter in thin InP membranes bonded with BCB on silicon. The measured losses are below $15\ \text{dB/cm}$ for the wires and the $3\ \text{dB}$ -splitter has only $0.6\ \text{dB}$ excess losses. The fabricated ring resonators showed a free spectral range of $28\ \text{nm}$ and a loaded Q-factor over $5,000$. Some of the rings showed Q values over $15,000$ together with propagation losses of $7\ \text{dB/cm}$. These values of Q are high enough to ensure lasing action with active material. We could also observe a non-linear behavior of these rings for an increasing input power, leading to bistability.

We believe that this IMOS (InP Membrane On Silicon) strategy is particularly attractive for very complex PICs working at telecom wavelengths as it could allow the integration of active and passive devices at the same level

References

- 1 G. Roelkens et al., J. Electrochem. Soc. **153**, G1015 (2006).
- 2 F. Bordas et al., Proc. ECIO'08, p.95 (2008).
- 3 D. Taillaert et al., Jpn. J. Appl. Phys. **45**, p.6071 (2006).
- 4 F. Van Laere et al., J. Lightwave Technol. **25**, p.151 (2007).
- 5 P. Dumon et al., IEEE Photon. Technol. Lett. **16**, p.1328 (2008).
- 6 M. Lesecq et al., IET Optoelectron. **2**, p.69 (2008).
- 7 M. Carette et al., Electron. Lett. **44** (2008).
- 8 G. Priem et al., Opt. Express **13**, p.9323 (2005).
- 9 G. Roelkens et al., J. Appl. Phys. **104**, 033117 (2008).